

Capture-Cross-Section Studies for 30–220-keV Neutrons Using a New Technique*

R. L. MACKLIN AND J. H. GIBBONS

Oak Ridge National Laboratory, Oak Ridge, Tennessee

(Received 27 February 1967)

Neutron-radiative-capture cross sections have been measured at various energies from 30–220 keV using a new “total-energy-detector” technique of high sensitivity, applicable to small samples of separated stable isotopes. Samples studied are: V, Fe, Ni, ^{86}Sr , ^{87}Sr , Y, Nb, Rh, Ag, ^{122}Te , ^{123}Te , ^{124}Te , ^{126}Te , ^{128}Te , ^{128}Te , ^{130}Te , I, Eu, ^{175}Lu , ^{176}Lu , W, Au, ^{204}Pb , and ^{208}Pb . The odd-odd isotope ^{176}Lu shows a substantially higher cross section than those of neighboring odd-even and even-odd nuclei. The results for europium (2 b near 65 keV) emphasize the peak expected from previous studies of systematics. The Sr and Te isotopic results strongly confirm the predictions of s-process stellar nucleosynthesis.

I. INTRODUCTION

THE study of neutron-capture cross sections has had three principal motivations: nuclear-reaction theory, stellar-nucleosynthesis theory, and nuclear-reactor design. The first two of these and, for special applications, the third have called for the study of specific individual isotopes. As the separation of isotopes is expensive and difficult, there has been continuing interest in increased sensitivity of measurement.

In the 10–300-keV neutron-energy range where much of the astrophysical and fast-breeder reactor interest in capture lies at present, techniques have progressed from simple activation techniques to large liquid scintillators,^{1–3} the lead slowing-down-time spectrometer,⁴ and most recently the Moxon-Rae detector.^{5,6} Each has offered advances in applicability, sensitivity, resolution, or insensitivity to details of the cascade of individual γ rays following neutron capture. The Moxon-Rae detector represented a new approach to this last point, achieving an *over-all* efficiency for capture γ rays *proportional to total energy* released (neutron energy plus binding energy) for energies from a few hundred keV to 10 MeV. The energy range over which the proportionality holds includes almost all the individual γ -ray energies resulting from neutron capture in nuclei. The low efficiency (typically a few percent) was more than compensated for by the fast time resolution (2×10^{-9} sec) possible and much useful work is still being done with this type detector.

Maier-Leibnitz has shown^{7,8} that for a wide class of

radiation detectors one can *generate* an average response function *proportional to energy* (or other parameters). This is done by applying a weighting function to each pulse from the detector which is a function of the pulse size only. Thus one must measure and record (or calculate a weight with) the pulse-height spectrum. However, one then has considerable freedom in optimizing the detector for efficiency, time resolution, insensitivity to scattered neutron backgrounds, etc.

II. EXPERIMENTAL

The ORNL 3-MV pulsed, bunched Van de Graaff with a thin ^7Li target was used as the neutron source as in earlier work.⁹ The neutrons near 0° were collimated by a channel through ^6LiH , $^6\text{Li}_2\text{CO}_3$ paraffin, and lead shielding (see Fig. 1). The neutron beam covered a transverse sample area about 2.5 cm wide by 7.5 cm high at a flight path of 51 cm. A ^{10}B slab at 135 cm viewed by a NaI(Tl) crystal was used as a neutron monitor. The monitor was corrected for background by time gating as in the total cross-section work,^{9,10} and for the few percent attenuation by the capture samples (calculated from the total cross section for each sample).

For time-of-flight measurements in the 5–100 keV neutron energy range we originally chose plastic scintillators rather than NaI(Tl) crystals for their fast time resolution (about 1 nsec) and low-neutron capture. However, moderation of scattered neutrons in the plastic gave an additional small background as these slow neutrons were captured near the detector. Later we bypassed this complication by using a nonhydrogenous liquid scintillator¹¹ (4 cm thick by 10 cm diameter). For the smallest cross sections (highest scattering to total ratio), we have also interposed 2.5-cm ^6LiH neutron shields between sample and detector to further reduce sensitivity to scattered neutrons. Weighting functions for this case were found by treating the shield as an inactive region of the detector.

* Research sponsored by the U. S. Atomic Energy Commission under contract with the Union Carbide Corporation.

¹ B. C. Diven, J. Terrell, and A. Hemmendinger, Phys. Rev. **120**, 556 (1960).

² J. H. Gibbons, R. L. Macklin, P. D. Miller, and J. H. Neiler, Phys. Rev. **122**, 182 (1961).

³ N. V. Kononov *et al.*, J. Nucl. Phys. USSR **4**, 282 (1966).

⁴ A. A. Bergman *et al.*, Conference on the Study of Nuclear Reactions with Neutrons, Antwerp, 1965 (unpublished), and earlier papers.

⁵ M. C. Moxon and E. R. Rae, in *Neutron Time-Of-Flight Methods*, edited by J. Spaepen (European Atomic Energy Committee, Brussels, 1961).

⁶ R. L. Macklin, J. H. Gibbons, and T. Inada, Nucl. Phys. **43**, 353 (1963).

⁷ H. Maier-Leibnitz (private communication).

⁸ F. Rau, Nucleonik **5**, 191 (1963).

⁹ R. L. Macklin, P. J. Pasma, and J. H. Gibbons, Phys. Rev. **136**, B695 (1964).

¹⁰ J. H. Gibbons and R. L. Macklin, Phys. Rev. **153**, 1356 (1967).

¹¹ Nuclear Enterprises Ltd.: NE-226.

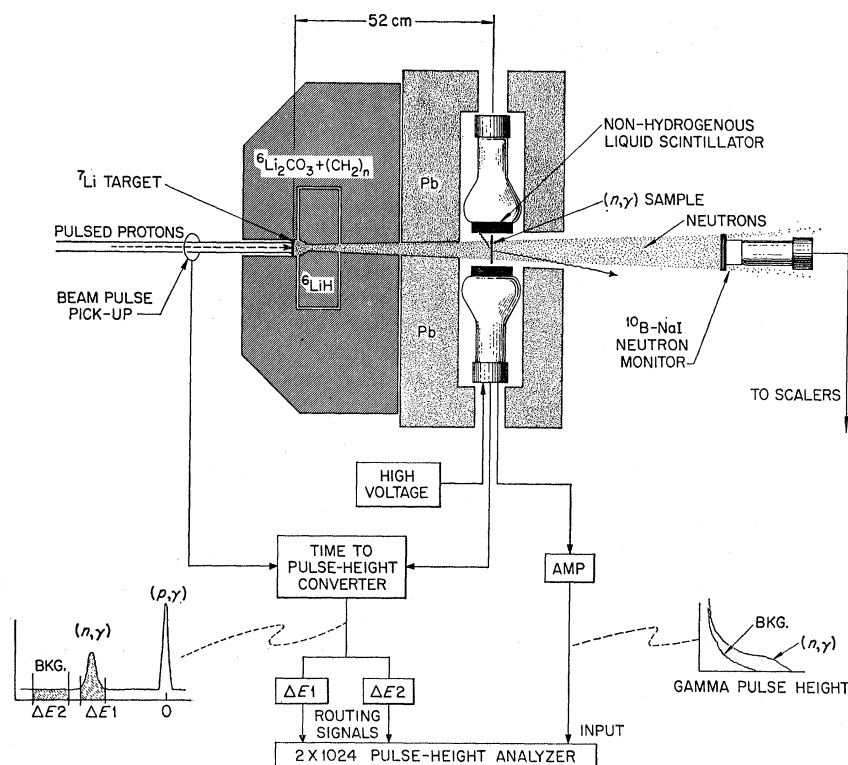


FIG. 1. Experimental arrangement using the "total-energy detector." The pulsed proton beam makes neutrons [${}^7\text{Li}(p,n){}^7\text{Be}$] which, after collimation, pass through the sample. The relatively rare-capture events are signaled by prompt-capture γ rays. The pulsed-beam technique is used to sort out events in time.

A symmetric pair of detectors was used primarily to get high-solid angle and low sensitivity to the exact sample placement between them. The larger detector efficiency of the "total energy detector" scheme results in a no longer negligible probability of detection of more than 1γ per capture. Such events must be corrected for since the pulse-height transformation is valid only for single γ rays. Because of the symmetry the summing between crystals is just equal to the summing within crystals assuming uncorrelated γ -ray directions or γ - γ angular correlations symmetric about 90° [even Legendre polynomials $P_{2n}(\cos\theta)$ only]. This last condition is generally fulfilled for neutron-capture cascades as the γ -emitting levels are not of mixed parity. Thus by arranging the pulse-height analyzer to subtract coincident pulses from the single-crystal spectra, the entire summing effect can be removed even for capture cascades.¹² For 4 γ rays of 1.86 MeV in the geometry mentioned above, summing without coincidence subtraction would lead to an 11% overestimate of the total energy. For typical neutron-capture cascades it might be half as much (6%). This is in comparison to single γ rays whose energy is given correctly (on the average) by the weighting factors. An outline of the calculation of the weighting functions is included in the Appendix.

While the efficiency for these detectors is high (40–50% per capture for 7.5-cm \times 10-cm-diam plastic) the

counting statistics after applying the weighting factors are poorer because the relatively rare pulses at large amplitudes are more heavily weighted. Fortunately for typical capture cascades the standard deviation error as computed from simple counting statistics is increased by only a small factor: 1.2–1.6 in the cases studied here.

Samples included enriched isotopes¹³ of strontium, tellurium, lutecium, and lead. The standard shape was 2.56 \times 2.56 cm, two of these being placed one above the other when sufficient material was available. The strontium samples were 5-cm-diam SrCO_3 pressings. The cross-section standard was tantalum, though in a few cases indium or iodine (PbI_2) was used as an intermediate reference. The tantalum standard cross section was taken as $8100E^{-0.697}$ mb for E in the range 20–220 keV. This function fitted the data of Ref. 2 and also more recent results.⁹ The cross section ratio of tantalum and indium was reinvestigated and found essentially constant over the neutron energy range 20–207 keV with the indium cross-section 6% higher. Approximately matching carbon samples were included in each data set to provide a measure of the backgrounds.

Calculated corrections were applied for the following sample effects: (a) neutron scattering and resonance self-protection¹⁴; (b) γ -ray attenuation; (c) binding plus kinetic energy (affects detector efficiency). The observed cross sections for enriched isotopic samples were

¹² Dr. Peter Armbruster has pointed out that this procedure slightly biases the shape of the derived singles spectrum. We have corrected the net counts for the measured coincidence loss.

¹³ Prepared by the Oak Ridge National Laboratory Isotopes Division.

¹⁴ R. L. Macklin, Nucl. Instr. Methods 26, 213 (1964).

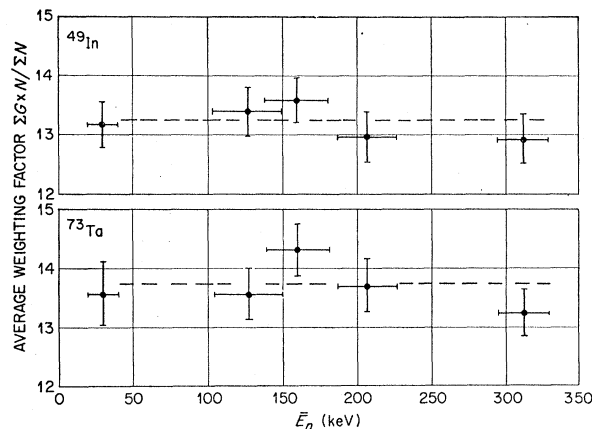


FIG. 2. Dependence of the average-pulse-height weighting factor as a function of captured neutron energy. These results, for samples of indium and tantalum, show the remarkable and fortuitous lack of sensitivity of the detector weighting factors on changes in capture cascades (such as are expected over this energy interval). To first order we see no dependence of the weighting factor on neutron energy.

corrected for isotopic impurities by an iterative unscrambling code. Inelastic scattering γ rays need to be corrected for at slightly higher-neutron energies than those used here (indium, for example).

III. RESULTS AND DISCUSSION

A. Detector Characteristics

The use of a γ detector with essentially no full energy peak appears to have been an *advantage* in this application. The capture-cross-section results turn out to be surprisingly insensitive to the weighting function. This is demonstrated most dramatically by comparing the (properly) weighted counts with the raw, unweighted ones.

The experimental results given in Fig. 2 show the insensitivity of the pulse-height distribution from the detectors to typical changes in γ -ray-cascade characteristics for two samples (Ta and In). Similar results were found for other samples. As the neutron energy is changed over the range indicated (30–300 keV) the neutron-capture reaction changes from predominantly $l=0$ (for the tantalum especially) through $l=1$ to $l=2$ with corresponding reversals of parity and changes of allowed spins (J 's) of the compound states. At the highest energy (312 keV) a few percent of the emitted γ -ray energy also comes from inelastic scattering to levels near 137 keV in the case of the tantalum.

The suggestion of higher ratios of net counts weighted for total energy to unweighted counts near 160 keV (and lower at 312 keV) is probably due to slight shifts in electronic threshold bias (below 40-keV equivalent pulse height) rather than any nuclear phenomenon.

Figure 3 indicates the dependence of the average weighting factor on the total γ energy released per capture for various isotopes. The near constancy above

7 MeV might correspond to a linear dependence of multiplicity on total energy with no change in the energy distribution of individual cascade γ rays. The apparent decrease in average weighting factor at lower energies corresponds to systematic changes in both multiplicity and γ -energy distribution. The dashed line shows an empirical linear dependence of average weighting factor on total energy release per neutron capture, apparently significant below about 7.5 MeV.

In view of the insensitivity of the results to the shape of the weighting-function versus pulse-height curve, the use of an analog circuit for on-line weighting might be suggested, which would obviate the necessity for multiparameter recording in experiments where more than one neutron energy is studied at one time.

B. Cross Sections

The cross-section results for samples where no individual resonance effects are evident are given in Table I. The combined-capture area for the two resonances at about 70 and 77 keV in ^{208}Pb was also detected. We found 375_{-250}^{+125} b eV, where the larger error bound corresponds to a possible contribution from scattered neutrons. If we assume the two resonances have $l=1$, $J=\frac{3}{2}$ (70 keV), $J=\frac{1}{2}$ (77 keV)¹⁰ and equal radiative widths, the common radiative width found is $2.2_{-1.5}^{+0.7}$ eV.

The capture values for iron and nickel span resonances (near 150 keV) known from total cross-section results but cannot be assigned to the known resonances exclusively as $l>0$ resonances are not resolved in the total cross-section work in this energy range.

The other elemental cross sections generally fall within the range of previous data, contributing new, independent support toward increased confidence in

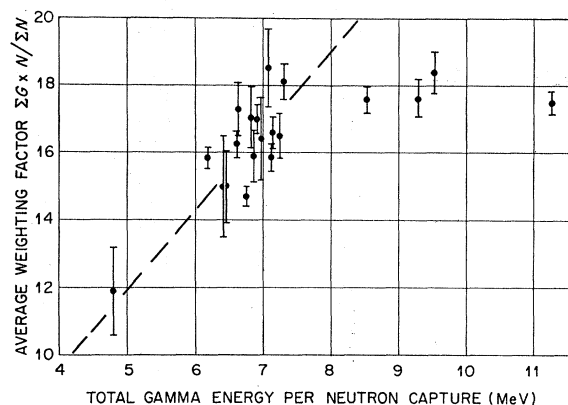


FIG. 3. Dependence of the average-pulse-height weighting factor on binding energy of the target nucleus plus a neutron. The dashed curve is the behavior expected from a simple model which assumes an energy dependence of the average-cascade γ on total binding energy. The near constancy of the data for energies greater than 7 MeV would be expected if for these energies the average-cascade γ energy was constant and multiplicity was the only variable.

TABLE I. Experimental results. Columns correspond to element and isotope, average neutron energy (keV), neutron energy spread (keV, full width at half-maximum), capture cross section (mb), and standard deviation error (mb) which includes the uncertainty in the standard cross section.

Element	Mass	\bar{E}_n (keV)	FWHM (keV)	σ_c (mb)	Std. dev. (mb)	Element	Mass	\bar{E}_n (keV)	FWHM (keV)	σ_c (mb)	Std. dev. (mb)
²³ V		104	15	5.5	1.2	⁵² Te	125	30	10	515.0	31.3
		125	23	4.1	1.4			30	10	459.5	30.2
		150	21	6.9	2.3			50	10	364.0	24.5
		182	21	7.6	2.3			70	19	222.9	11.6
²⁶ Fe		125	23	7.2	1.5	85	17	198.3	24.2		
		150	21	12.4	3.0	125	23	126.1	8.9		
		182	21	6.5	2.6	30	10	90.5	10.5		
						30	10	94.3	11.3		
²⁸ Ni		125	23	14.1	1.5	50	10	63.6	6.9		
		150	21	29.2	3.0	70	19	46.3	5.1		
		182	21	12.6	2.6	85	17	42.6	11.6		
						125	23	23.9	3.3		
³⁸ Sr	86	30	10	74.0	6.8	128	30	10	43.6	8.4	
		65	20	35.1	3.3		30	10	20.4	6.8	
		125	23	28.9	2.4		50	10	20.4	5.1	
	87	30	10	108.7	8.9	70	19	24.4	4.5		
		65	20	56.0	4.5	85	17	12.7	9.5		
		125	23	37.6	2.9	125	23	12.6	3.3		
³⁹ Y		70	19	12.7	2.3	130	30	10	10.0	6.9	
		85	17	7.7	2.4		30	10	17.8	7.1	
		104	15	13.0	4.1		70	19	12.1	3.8	
		125	23	6.5	2.4		85	17	-2.4	8.1	
		150	21	7.7	3.6		125	23	6.0	3.3	
		182	21	13.8	4.1						
⁴¹ Nb		70	19	168.4	7.4	⁵³ I	125	23	234.7	17.4	
		85	17	130.1	8.0		150	21	183.6	28.8	
		104	15	119.0	8.9		182	21	202.5	28.1	
		125	23	118.3	7.2		⁶³ Eu	30	10	3372.9	234.7
		150	21	83.0	7.8			50	10	2228.5	153.1
		182	21	77.0	5.9			70	19	1983.7	127.3
				85	17	1633.1		122.2			
				104	15	1446.2		112.6			
				125	23	1169.4		93.9			
⁴⁵ Rh		70	19	708.1	25.7	200	20	769.7	83.3		
		125	23	415.5	15.9	⁷¹ Lu	175	30	1410.9	107.0	
		150	21	353.3	26.3		50	10	1033.3	80.9	
		182	21	336.7	23.3		70	19	850.6	67.9	
							85	17	721.2	54.8	
				104	15		677.1	54.7			
⁴⁷ Ag		104	15	434.5	30.5	125	23	578.5	47.5		
		125	23	405.4	15.0	157	21	429.7	48.6		
		150	21	342.3	24.8	200	20	364.5	43.8		
		182	21	310.5	21.5	176	30	10	2245.6	170.3	
							50	10	1588.3	121.1	
				70	19		1179.6	92.6			
				85	17		1075.1	80.5			
				104	15		927.7	73.8			
⁵² Te	122	30	10	168.9	33.5	125	23	825.2	67.1		
		30	10	183.2	32.3	157	21	757.7	81.5		
		50	10	181.7	25.5	200	20	769.0	85.1		
		70	19	147.0	19.2	⁷⁴ W	125	23	129.5	8.1	
		85	17	116.2	43.1		150	21	124.0	14.7	
		104	15	103.1	19.8		182	21	90.4	11.9	
		125	23	96.7	13.0		220	20	88.0	13.5	
	123	30	10	803.2	58.8		⁷⁹ Au	125	23	272.5	15.3
		30	10	703.0	49.4			150	21	252.5	18.2
		50	10	562.3	44.4			182	21	230.6	15.9
	124	70	19	485.5	34.1	⁸² Pb	204	30	42.6	5.4	
		104	15	318.3	29.1		50	10	31.9	3.3	
		125	23	319.8	23.9		85	17	35.6	4.0	
		30	10	134.5	15.9		104	15	27.6	3.7	
30		10	116.5	14.3	157		21	25.4	6.4		
50		10	119.0	12.6							
70		19	92.8	9.6							

“evaluated” cross section curves required for computer calculations of nuclear reactor designs. In the case of gold where the spread of previous results has ap-

proached a factor of 2 in the 20–80-keV range, the present values continue to support the low results of Ref. 2, albeit the present results are in the range 125–182

keV where the spread in previously reported values is a bit smaller than at lower energies.

The rare-earth samples show significantly higher cross sections than we found previously.² The europium oxide¹⁵ and lutetium isotope oxides represent much smaller and perhaps purer samples than were used in our earlier studies.

The odd-odd ¹⁷⁶Lu shows especially enhanced neutron capture. In Ref. 2 it was suggested that an odd number of total nucleons in the target (hence an even number in the compound nucleus) corresponded to an enhancement of about a factor of 2.2 in compound nucleus level density and hence capture cross section over that of even-even targets. The ¹⁷⁶Lu result can be understood as an extension of this empirical rule such that either an odd number of neutrons or an odd number of protons in the target (hence even neutron number but odd proton number in the compound nucleus) independently correspond to such an enhancement factor. ¹⁷⁶Lu exhibits a neutron-capture cross section 1.6 times higher than the neighboring ¹⁷⁵Lu.

The results on individual isotopes of strontium and tellurium are of considerable interest in the study of the "s process" stellar nucleosynthesis of heavy elements.¹⁶⁻¹⁸ The s-process theory predicts highly quantitative correlations between isotopic abundance and capture cross section (for Maxwellian neutrons with $kT \sim 30$ keV) for certain nuclides. The results reported here are in very good agreement with s-process predictions and are discussed in detail elsewhere.¹⁹ Tellurium is the *only* element in which more than two isotopes were generated solely by the s process and it therefore is a sensitive test. The strontium results are particularly interesting because in this region of atomic weight nuclear-shell effects strongly affect the relative production of elements in stars and consequently the predicted correlation between cross section and abundance.

IV. CONCLUSIONS

The total-energy-detector technique offers increased efficiency, low backgrounds, and good time resolution for neutron-capture cross section measurements. Efficiencies above 20%, including solid angle, for samples down to 3 g (¹²²Te) at an over-all resolution of $\sim 2 \times 10^{-9}$ sec (~ 4 nsec/meter) have been obtained. Application of the technique for conventional time-of-flight work (simultaneous measurement of cross sections over a range of energies) will require two-dimensional analysis or on-line pulse-height weighting. The results of keV-range capture cross sections tend to support our earlier

reported values at lower energies and extend many to higher energies. The results using selected isotopes give further confirmation to the "s process" of stellar nucleosynthesis of certain heavy elements.

APPENDIX

A few properties of total-energy weighting functions can be visualized for idealized detectors. If all the energy of every γ -ray incident could be converted to pulse height (100% peak efficiency) the weighting factor becomes directly proportional to the pulse height and inversely proportional to the solid-angle factor ($\Omega/4\pi$). This case is approximated by a large NaI(Tl) crystal with the γ rays collimated for incidence at the bottom of a well in the crystal. A proportionate resolution broadening leaves the weighting function unchanged.

For a pulse-height response uniformly distributed up to the incident energy (similar to proton-recoil-detector response for neutrons) the weighting function contains merely an additional constant factor of 2. If the total detection efficiency is falling off as $(E_\gamma)^{-k}$ [similar to the $H(n,n)$ cross section from 0.015–5 MeV for $k=1$ or the Compton cross section from 0.5–10 MeV for $k=0.5$] the weighting factor becomes proportional to $(E_\gamma)^{k+1}/(\Omega/4\pi)$. For practical detectors we thus expect a weighting factor rising more rapidly than pulse height but not so rapidly as the square of the pulse height. Modifications due to multiple interactions and electron escape, to mention two of the largest effects, should be minor.

For use with the ORNL 3-MV pulsed Van de Graaff, a detector with time resolution approaching 1 nsec, is the most important consideration. Plastic scintillators seemed best for this reason, although their γ -detection efficiency is low, being dominated by the Compton process. As the Compton cross section is well understood²⁰ a code was written to calculate the pulse-height distributions from right circular cylinders of plastic scintillator for γ rays of given energy up to 10 MeV in 50-keV steps. The first interaction was integrated channel by channel using the differential cross section, and including the loss of electrons which leave the crystal (wall effect). Paths penetrating the rear face of the crystal led to exponential integrals; those intersecting the curved sides were integrated numerically. Multiple Compton interactions were followed by taking the average Compton scattered γ -ray energy (and its angle) at each step with a typical path length until the residual γ energy was 25 keV. As the carbon photoelectric cross section rises steeply below 25 keV and is comparable to the Compton cross section there, it was convenient to terminate the multiple Compton scattering at 25 keV with a photoelectric interaction. Although it took about 20 multiple scatterings to degrade the residual γ energy to 25 keV, scatterings beyond the third were hardly

¹⁵ Kindly loaned by V. E. Hampel of Lawrence Radiation Laboratory, Livermore, California.

¹⁶ E. M. Burbidge, G. R. Burbidge, W. A. Fowler, and F. Hoyle, *Rev. Mod. Phys.* **29**, 547 (1957).

¹⁷ R. L. Macklin and J. H. Gibbons, *Rev. Mod. Phys.* **37**, 166 (1965).

¹⁸ P. A. Seeger, W. A. Fowler, and D. D. Clayton, *Astrophys. J. Suppl.* **97**, 121 (1965).

¹⁹ R. L. Macklin and J. H. Gibbons, *Astrophys. J.* (to be published).

²⁰ A. T. Nelms, *Natl. Bur. Std. (U. S.), Circ. No. 542* (1953).

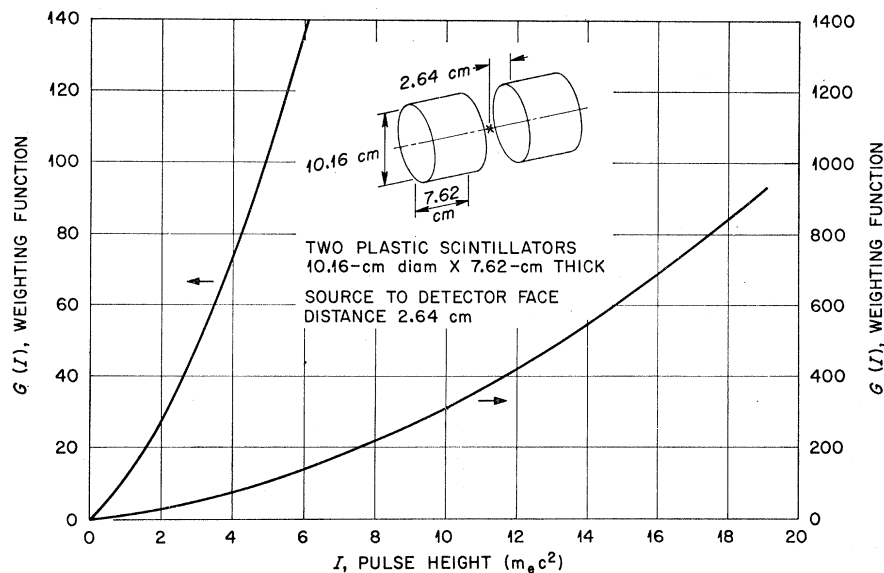


FIG. 4. Dependence of the pulse-height weighting function $G(I)$ upon pulse height for the detectors shown in the figure.

significant. The (small) pair-production cross section was also included in the calculation with its own wall effect treated approximately and the multiple Compton interactions of its annihilation quanta included.

From the computed pulse-height spectra $[P(I, E)]$, weighting functions $G(I)$ were found from a chain of equations⁷

$$\sum G(I)P(I, E_\gamma) = E_\gamma, \quad (1)$$

where I is a pulse height channel number. It was hoped that the inclusion of the tiny full-energy tail would lead to a smooth solution. As noted in Ref. 8, however, severe oscillations were found for increasing E_γ until the secondary Compton γ -rays were treated channel by channel (rather than as a single average), the pair peaks broadened over seven channels (with a nearly Gaussian resolution function) and pulses above the Compton edge replaced by ones at the Compton edge plus an equal number drawn symmetrically from below the Compton edge. This last procedure is the inverse of resolution broadening and allowed the sharp discontinuity at the Compton edge E_c to terminate the distribution, the $G(I)$ then being found from

$$\sum G(I)P(I, E_c) = E_\gamma. \quad (2)$$

The above procedure can be iterated using the weighting function found at the first (preceding) step. This is considered an improvement on the usual practice of discarding the high-energy tails of the pulse spectra. The weighting-factor oscillation was reduced to about 2% near 10 MeV and the $G(I)$ were smoothed by a

least-squares-fitting function of the form

$$G(X) = (0.95X + 0.021X^2) / (1.09 - 4.3 \times 10^{-3}X + 4.4 \times 10^{-5}X^2 - 1.2 \times 10^{-7}X^3), \quad X \text{ in } 0.1m_e c^2 \text{ units.} \quad (3)$$

The constants in Eq. (3) were for a pair of 10-cm-diam \times 7.5-cm-thick detectors with an isotropic point source between them on their common axis 2.10 cm from each (see Fig. 4). Deviations up to $\pm 12\%$ were found in the first few channels but no more than a 3.3% deviation was found from channels 5–190. As the fitting function is used to interpolate the weighting functions for the 20 channels or so used in a particular experiment it was not felt necessary to go to a finer grid (i.e., more than 190 channels per 10 MeV).

For the pair of 10-cm-diam 4-cm-thick NE-226 hydrogen free liquid scintillator cells, each 1.8 cm from a source point we found:

$$G(X) = (0.49X + 0.00963X^2 - 1.22 \times 10^{-5}X^3) / (1.047 - 4.681 \times 10^{-3}X + 9.437 \times 10^{-5}X^2 - 6.270 \times 10^{-7}X^3 + 1.39 \times 10^{-9}X^4). \quad (4)$$

The effect of the glass cell wall is included in (3) and (4). Adding 3-cm ${}^6\text{LiH}$ shields between source and (hydrogen-free) detector (thus increasing the distance from the source to the face of each detector to 4.8 cm) gave

$$G(X) = (0.80X + 0.02075X^2 - 5.97 \times 10^{-5}X^3) / (1.0340 - 4.373 \times 10^{-3}X + 7.131 \times 10^{-5}X^2 - 5.063 \times 10^{-7}X^3 + 1.10 \times 10^{-9}X^4).$$